

Self-supervised Video Representation Learning by Uncovering Spatio-temporal Statistics

Jiangliu Wang*, Jianbo Jiao*, *Member, IEEE*, Linchao Bao, Shengfeng He, *Member, IEEE*, Wei Liu, *Senior Member, IEEE* and Yun-hui Liu, *Fellow, IEEE*

Abstract—This paper proposes a novel pretext task to address the self-supervised video representation learning problem. Specifically, given an unlabeled video clip, we compute a series of spatio-temporal statistical summaries, such as the spatial location and dominant direction of the largest motion, the spatial location and dominant color of the largest color diversity along the temporal axis, *etc.* Then a neural network is built and trained to yield the statistical summaries given the video frames as inputs. In order to alleviate the learning difficulty, we employ several spatial partitioning patterns to encode rough spatial locations instead of exact spatial Cartesian coordinates. Our approach is inspired by the observation that human visual system is sensitive to rapidly changing contents in the visual field, and only needs impressions about rough spatial locations to understand the visual contents. To validate the effectiveness of the proposed approach, we conduct extensive experiments with several 3D backbone networks, *i.e.*, C3D, 3D-ResNet and R(2+1)D. The results show that our approach outperforms the existing approaches across the three backbone networks on various downstream video analytic tasks including action recognition, video retrieval, dynamic scene recognition, and action similarity labeling. The source code will be made publicly available at: https://github.com/laura-wang/video_repres_sts.

Index Terms—Self-supervised Learning, Representation Learning, Video Understanding, 3D CNN.

1 INTRODUCTION

POWERFUL video representations serve as the foundations for solving many video content analysis and understanding tasks, such as action recognition [1], [2], video retrieval [3], [4], video captioning [5], [6], *etc.* Various network architectures [1], [7], [8] are designed and trained with massive human-annotated video data to learn video representations for individual tasks specifically. While great progresses have been made, supervised video representation learning is impeded by two major obstacles: (1) Annotation of video data is labour-intensive and expensive, thus restricting supervised learning to relish a large quantity of free video resources on the Internet. (2) Representations learned from labeled video data lack generality and robustness, *e.g.*, video features learned for action recognition do not well to video retrieval task [9], [10].

To tackle the aforementioned challenges, multiple approaches [11], [12], [13], [14] have emerged to learn more generic and robust video representations in a self-supervised manner. Neural network are first pre-trained with unlabeled videos using some *pretext tasks*, where supervision signals are derived from input data without human annotations. Then the learned representations can be

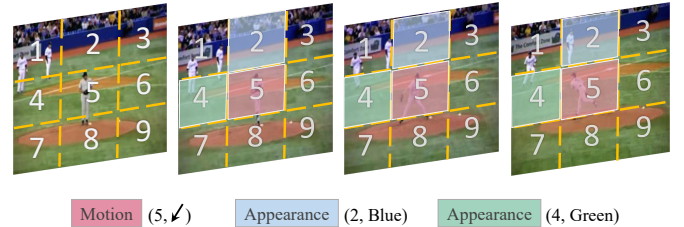


Fig. 1: The main idea of the proposed approach. Given a video sequence, we design a pretext task to regress the summaries derived from spatio-temporal statistics for video representation learning without human-annotated labels. Each video frame is first divided into several spatial regions using different partitioning patterns like the grid shown in the figure. Then the derived statistical labels, such as *the region with the largest motion and its direction* (the red patch), *the most diverged region in appearance and its dominant color* (the blue patch), and *the most stable region in appearance and its dominant color* (the green patch), are employed as supervision signals to guide the representation learning.

employed as weight initialization for training models or be directly used as features in succeeding *downstream tasks*.

Among the existing self-supervised video representation learning methods, video order verification/prediction [11], [12], [13], [14], [15] is one of the most popular pretext tasks. It randomly shuffles video frames and asks a neural network to predict whether the video is perturbed or to rearrange the frames in a correct chronological order. By utilizing the intrinsic temporal characteristics of videos, these pretext tasks have been shown useful for learning high-level semantic features. However, the performances of these approaches are limited since the contents of individual frames are mostly unexploited during learning. Other

- J. Wang and Y. Liu are with the CUHK T Stone Robotics Institute, The Chinese University of Hong Kong. Email: {jlwang, yh-liu}@mae.cuhk.edu.hk.
- J. Jiao is with the Department of Engineering Science, University of Oxford. Email: jianbo@robots.ox.ac.uk.
- L. Bao and W. Liu are with Tencent AI Lab. Email: {linchaobao@gmail.com, wl2223@columbia.edu}
- S. He is with the School of Computer Science and Engineering, South China University of Technology. Email: shengfenghe7@gmail.com.
- J. Wang and J. Jiao contributed equally to this work. L. Bao and Y. Liu are the corresponding authors.

Preprint. Under review.

approaches include flow fields prediction [16], future frame prediction [17], [18], [19], dense predictive coding [20], *etc.* Although promising results have been achieved, the above mentioned pretext tasks may lead to redundant feature learning towards solving the pretext task itself, instead of learning generic representative features for downstream video analytic tasks. For example, predicting the future frame requires the network to precisely estimate each pixel in each frame in a video clip. This increases the learning difficulties and causes the network to waste a large portion of the capacity on learning features that may be not transferable to high-level video analytic tasks.

In this paper, we argue that a pretext task should be intuitive and relatively simple to learn, enlightened by the human visual system, and mimicking the video understanding process of humans. To this end, we propose a novel pretext task to learn video representations by regressing spatio-temporal statistical summaries from unlabeled videos. For instance, given a video clip, the network is encouraged to identify the largest moving area with its corresponding motion direction, as well as the most rapidly changing region with its dominant color. The idea is inspired by the cognitive study on human visual system [21], in which the representation of motion is found to be based on a set of learned patterns. These patterns are encoded as sequences of snapshots of body shapes by neurons in the *form pathway*, and by sequences of complex optic flow patterns in the *motion pathway*. In our work, these two pathways are defined as the appearance branch and motion branch, respectively. In addition, we define and extract several abstract statistical summaries accordingly, which is also inspired by the biological hierarchical perception mechanism [21].

We design several spatial partitioning patterns to encode each spatial location and its spatio-temporal statistics over multiple frames, and use the encoded vectors as supervision signals to train the neural network for spatio-temporal representation learning. The novel objectives are simple to learn and informative for the motion and appearance distributions in videos, *e.g.*, the spatial locations of the most dominant motions and their directions, the most consistent and the most diverse colors over a certain temporal cube, *etc.* An illustration of the main idea is shown in Fig. 1, where a 3×3 grid pattern with motion and appearance statistics is shown for example. We conduct extensive experiments with 3D convolutional neural networks to validate the effectiveness of the proposed approach. The experimental results show that, compared with training from scratch, pre-training using our approach demonstrates a large performance gain for video action recognition problem (*e.g.*, 56.0% *vs.* 77.8% on UCF101 and 22.0% *vs.* 40.5% on HMDB51). By transferring the learned representations to other video tasks, such as video retrieval, dynamic scene recognition, *etc.*, we further demonstrate the generality and robustness of the video representations learned by the proposed approach.

A preliminary version of this work was presented in [22], where the basic idea of utilizing spatio-temporal statistical information for video representation learning is introduced. In this paper, we extend the previous work in the following aspects: *First*, we provide a more detailed implementation of the proposed self-supervised learning approach and add thorough ablation studies on a large-scale dataset kinetics-

400 to explore the relationship between training data size and downstream task performance. *Second*, we extend the proposed method to more backbone networks, *i.e.*, C3D with BN, 3D-ResNet and R(2+1)D. Detailed ablation studies are conducted to investigate whether the performance enhancement comes from the external network architectures or the internal self-supervised learning methods. *Third*, a curriculum learning strategy is introduced to further improve the representation learning. *Finally*, we further validate the proposed method on a new downstream task, video retrieval, to evaluate the generality of the video features.

To summarize, the main contributions of this work are four-fold: (1) We propose a novel pretext task for video representation learning by uncovering motion and appearance statistics without human annotated labels. Unlike prior pretext tasks [14], [17] that are even hard for humans to solve, the proposed tasks in our approach are consistent with human inherent visual habits and easy to learn. (2) We introduce a curriculum learning strategy based on the proposed spatio-temporal statistics, which is also inspired by the human learning process: from simple samples to difficult samples. (3) Extensive ablation studies are conducted and analyzed to reveal several insightful findings for self-supervised learning, including the effectiveness of training data scale, network architectures, and feature generalization, to name a few. (4) The proposed approach significantly outperforms previous approaches across all the studied network architectures in various video analytic tasks. Code and models will be made publicly available online.

The rest of this paper is organized as follows: First, we review relevant background knowledge and related work in Sec. 2. We then elaborate on the proposed statistics-based approach for self-supervised video representation learning in Sec. 3, where the quantified statistical labels and learning framework are introduced in detail. Following that, we introduce the experimental setup in Sec. 4, including datasets and implementation details. In Sec. 5, we seek to understand the effectiveness of the proposed method through comprehensive ablative analysis. Finally, we compare the proposed method with other state-of-the-art methods on several downstream tasks, including video action recognition, video retrieval, dynamic scene recognition, and action similarity labeling in Sec. 6. The whole work is concluded in Sec. 7 with possible future directions.

2 RELATED WORK

In this section, we briefly summarize the most related work to ours, including self-supervised representation learning and its applications on downstream video analytic tasks. Please refer to a recent survey [23] for more details.

2.1 Self-supervised Representation Learning

Self-supervised representation learning is proposed to leverage huge amounts of unlabeled data to learn useful representations for various problems, for example, image classification, object detection, human action recognition, *etc.* It has been proven that lots of deep learning methods can benefit from pre-trained models on large labeled datasets, *e.g.*, ImageNet [24] for image tasks and Kinetics [25] or

Sports-1M [26] for video tasks. The basic motivation behind self-supervised representation learning is to replace the extensively labeled data with “free” unlabeled data.

A common way to achieve self-supervised learning is to derive easy-to-obtain supervision signals without human annotations, to encourage the learning of useful features for downstream tasks. Various novel pretext tasks are proposed to learn image representations from unlabeled image data, *e.g.*, re-ordering perturbed image patches [27], [28], colorizing grayscale images [29], inpainting missing regions [30], counting virtual primitives [31], classifying image rotations [32], predicting image labels obtained using a clustering algorithm [33], *etc.* There are also studies that try to learn image representations from unlabeled video data. Wang and Gupta [34] proposed to derive supervision labels from unlabeled videos using traditional tracking algorithms. Pathak *et al.* [35] instead obtained labels from videos using conventional motion segmentation algorithms.

Recent studies leveraging video data try to learn transferable representations for video downstream tasks, such as action recognition, video retrieval, *etc.* Intuitively, a large number of studies [11], [12], [15] leveraged the distinct temporal information of videos and proposed to use frame sequence ordering as their pretext tasks. Büchler *et al.* [9] further used deep reinforcement learning to design a sampling permutations policy. Gan *et al.* [16] proposed a geometry-guided network that forces the CNN to predict flow fields or disparity maps between two consecutive frames. Although these work demonstrated the effectiveness of self-supervised representation learning with unlabeled videos and showed impressive performances when transferring the learned features to video recognition tasks, their approaches are only applicable to a CNN that accepts one or two frames as inputs and cannot be applied to network architectures that are suitable for spatio-temporal representations. Therefore, several recent papers [10], [13], [14], [20] used 3D CNNs as backbone networks to learn spatio-temporal representations, among which [10], [13], [14] extended the 2D frame ordering pretext tasks to 3D video clip ordering, and [20] formulated the pretext task as a dense prediction problem and proposed to predict future frames. Very recently, self-supervised learning leveraging multi-modality sources, *e.g.*, learning from video and audio [36], [37], is becoming increasingly popular. While note that in this paper, we focus on single modality, *i.e.*, only consider learning representations in the video domain.

2.2 Representation Learning for Video Analytic Tasks

Representation learning serves as the fundamental building block in tackling most video analytic tasks, such as complex action recognition [38], action detection and localization [39], [40], [41], video captioning [5], [6], *etc.* Two types of application modes are commonly adopted to evaluate the self-supervised video representation learning, either through transfer learning (as an initialization model) or feature learning (as a feature extractor).

Action recognition is one of the most widely used downstream video analytic tasks. At the beginning, researchers have developed various spatio-temporal descriptors for video representations to tackle this problem [42],

[43], [44]. While promising results are achieved by the best-performing hand-crafted feature-improved dense trajectories (iDT) descriptors [44], extensive efforts have been focusing on the deep neural networks development due to the impressive success achieved by CNN. Tran *et al.* [45] proposed C3D that extends the 2D kernels to 3D kernels to capture spatio-temporal video representations. Simonyan and Zisserman [7] proposed a two-stream network that extracts spatio and temporal features on RGB and optical flow inputs, respectively. Stemmed from these two works, various network architectures are designed to learn video representations, including P3D [46], I3D [1], R(2+1)D [8], *etc.* In this work, we consider to use three backbone networks, C3D [45], 3D-ResNet [8] and R(2+1)D [8] to validate the proposed approach, following prior works [10], [14]. Backbone networks pre-trained with the proposed spatio-temporal statistics will be used as weight initialization and fine-tuned on UCF101 [47] and HMDB51 [48] datasets for the action recognition downstream task.

The other kind of evaluation mode is to use the pre-trained networks as feature extractors for the downstream video analytic tasks, such as video retrieval [10], [11], [14], dynamic scene recognition [16], [49], *etc.* Without fine-tuning, such a mode can directly evaluate the generality and robustness of the learned features. Performances of the self-supervised methods are compared with both competitive hand-crafted video features, such as spatio-temporal interest points (STIP) [42], HOG3D [43], slow feature analysis (SFA) [50], Bags of Spacetime Energies (BoSE) [51], *etc.*, and other self-supervised learning methods.

3 OUR PROPOSED APPROACH

In this section, we first explain the high-level ideas and motivations for designing our novel pretext task with a simple illustration (Sec. 3.1). Next, we formally define the computation of the spatio-temporal statistical labels from the motion aspect (Sec. 3.2) and appearance aspect (Sec. 3.3), respectively. A curriculum learning strategy is presented in Sec. 3.4. Finally, we summarize the whole learning framework with 3D CNNs in Sec. 3.5.

3.1 Motivation

Inspired by human visual system, we break the process of video contents understanding into several questions and encourage a CNN to answer them accordingly: (1) Where is the largest motion in a video? (2) What is the dominant direction of the largest motion? (3) Where is the largest color diversity and what is its dominant color? (4) Where is the smallest color diversity, *e.g.*, the potential background of a scene, and what is its dominant color? The motivation behind these questions is that the human visual system [21] is sensitive to large motions and rapidly changing contents in the visual field, and only needs impressions about rough spatial locations to understand the visual contents. We argue that a good pretext task should be able to capture necessary representations of video contents for downstream tasks, while at the same time does not waste model capacity on learning too detailed information that is not transferable to other downstream tasks. To this end, we design our pretext

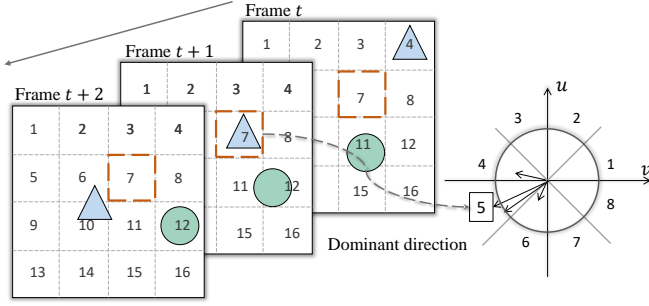


Fig. 2: The illustration of extracting statistical labels in a three-frame video clip. Detailed explanation is in Sec. 3.1.

task as learning to answer the above questions with only rough spatio-temporal statistical summaries, *e.g.*, for spatial coordinates we employ several spatial partitioning patterns to encode rough spatial locations instead of exact spatial Cartesian coordinates. In the following, we use a simple illustration to explain the basic idea.

Fig. 2 shows an example of a three-frame video clip with two moving objects (blue triangle and green circle). A typical video clip usually contains much more frames while here we use the three-frame clip example for a better understanding of the key ideas. To roughly represent the location and quantify “where”, each frame is divided into 4-by-4 blocks and each block is assigned to a number in an ascending order starting from 1 to 16. The blue triangle moves from block 4 to block 7, and the green circle moves from block 11 to block 12. Comparing the moving distances, we can easily find that the motion of the blue triangle is larger than the motion of the green circle. The largest motion lies in block 7 since it contains moving-in motion between frames t and $t + 1$, and moving-out motion between frames $t + 1$ and $t + 2$. Regarding the question “*what is the dominant direction of the largest motion?*”, it can be easily observed that in block 7, the blue triangle moves towards lower-left. To quantify the directions, the full angle 360° is divided into eight angle pieces, with each piece covering a 45° motion direction range, as shown on the right side in Fig. 2. Similar to location quantification, each angle piece is assigned to a number in an ascending order counterclockwise. The corresponding angle piece number of “lower-left” is 5.

The above illustration explains the basic idea of extracting statistical labels for motion characteristics. To further consider appearance characteristics “*where is the largest color diversity and its dominant color?*”, both block 7 and block 12 change from the background color to the moving object color. When considering that the area of the green circle is larger than the area of the blue triangle, we can tell that the largest color diversity location lies in block 12 and the dominant color is green.

Keeping the above ideas in mind, we next formally describe the approach to extract spatio-temporal statistical labels for the proposed pretext task. We assume that by training a spatio-temporal CNN to disclose the motion and appearance statistics mentioned above, better spatio-temporal representations can be learned, which will benefit the downstream video analytic tasks consequently.

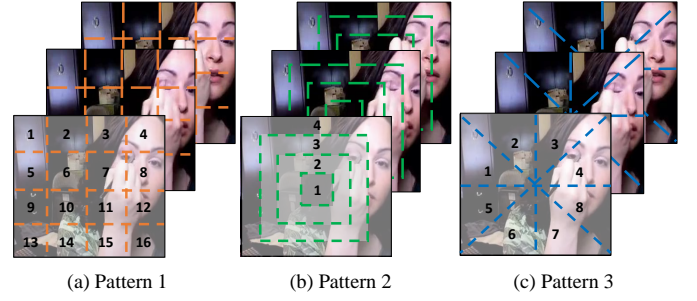


Fig. 3: Three different partitioning patterns used to divide video frames into different spatial regions. Each spatial block is assigned with a number to represent its location.

3.2 Motion Statistics

Optical flow is a commonly used feature to represent motion information in many action recognition methods [1], [7]. In the self-supervised learning paradigm, predicting optical flow between every two consecutive frames is leveraged as a pretext task to pre-train the deep model, *e.g.*, [16]. Here we also leverage optical flow estimated from a conventional non-parametric coarse-to-fine algorithm [52] to derive the motion statistical labels that are regressed in our approach.

However, we argue that there are two main drawbacks when directly using dense optical flow to compute the largest motion in our pretext task: (1) optical flow based methods are prone to being affected by camera motion, since they represent the absolute motion [53], [54]. (2) Dense optical flow contains sophisticated and redundant information for statistical labels computation, thus increasing the learning difficulty and leading to network capacity waste for self-supervised representation learning. To mitigate the influence from the above problems, we instead seek to use a more robust and sparse feature – motion boundary [53].

Motion Boundary. Denote the horizontal and vertical components of optical flow as u and v , respectively. Motion boundaries are derived by computing the x - and y -derivatives of u and v , respectively:

$$m_u = (u_x, u_y) = \left(\frac{\partial u}{\partial x}, \frac{\partial u}{\partial y} \right), m_v = (v_x, v_y) = \left(\frac{\partial v}{\partial x}, \frac{\partial v}{\partial y} \right), \quad (1)$$

where m_u is the motion boundary of u and m_v is the motion boundary of v . As motion boundaries capture changes in the flow field, constant or smoothly varying motion, such as motion caused by camera view change, will be cancelled out. Specifically, given an N -frame video clip, $(N - 1) * 2$ motion boundaries are computed based on $N - 1$ optical flows. Diverse video motion information can be encoded into two summarized motion boundaries by summing up all these $(N - 1)$ sparse motion boundaries m_u and m_v :

$$M_u = \left(\sum_{i=1}^{N-1} u_x^i, \sum_{i=1}^{N-1} u_y^i \right), M_v = \left(\sum_{i=1}^{N-1} v_x^i, \sum_{i=1}^{N-1} v_y^i \right), \quad (2)$$

where M_u denotes the summarized motion boundaries on horizontal optical flow u , and M_v denotes the summarized motion boundaries on vertical optical flow v .

Spatial-aware Motion Statistical Labels. Based on motion boundaries, we next describe how to compute the spatial-aware motion statistical labels that describe the largest motion location and the dominant direction of the largest motion. Given a video clip, we first divide it into

spatial blocks using partitioning patterns as shown in Fig 3. Here, we introduce three simple yet effective patterns: pattern 1 divides each frame into 4×4 grids; pattern 2 divides each frame into 4 different non-overlapped areas with the same gap between each block; pattern 3 divides each frame by two center lines and two diagonal lines. Then we compute summarized motion boundaries M_u and M_v as described in Eq. 2. Motion magnitude and orientation of each pixel can be obtained by casting M_u and M_v from the Cartesian coordinates to the Polar coordinates.

We take pattern 1 as an example to illustrate how to generate the motion statistical labels, while other patterns follow the same procedure. For the *largest motion location labels*, we first compute the average magnitude of each block, ranging from block 1 to block 16 in Pattern 1. Then we compare and find out block B with the largest average magnitude from the 16 blocks. The index number of B is taken as the largest motion location label. Note that the largest motion locations computed from M_u and M_v can be different. Therefore, two corresponding labels are extracted from M_u and M_v , respectively.

Based on the largest motion block, we compute the *dominant orientation label*, which is similar to the computation of motion boundary histogram (MBH) [53]. We divide 360° into 8 bins evenly, and assign each bin to a number to represent its orientation. For each pixel in the largest motion block, we use its orientation angle to determine which angle bin it belongs to and add the corresponding magnitude value into the angle bin. The dominant orientation label is the index number of the angle bin with the largest magnitude sum. Similarly, two orientation labels are extracted from M_u and M_v , respectively.

Global Motion Statistical Labels. We further propose global motion statistical labels that provide complementary information to the local motion statistics described above. Specifically, given a video clip, the model is asked to predict the frame index (instead of the block index) with the largest motion. To succeed in such a pretext task, the model is encouraged to understand the video contents from a global perspective. Motion boundaries m_u and m_v between every two consecutive frames are used to calculate the largest motion frame index accordingly.

3.3 Appearance Statistics

Spatio-temporal Color Diversity Labels. Given an N -frame video clip, we divide it into spatial video blocks by patterns described above, same as the motion statistics. For an N -frame video block, we compute the 3D distribution V_i in 3D color space of each frame i . We then use the Intersection over Union (IoU) along the temporal axis to quantify the spatio-temporal color diversity as follows:

$$\text{IoU}_{\text{score}} = \frac{V_1 \cap V_2 \cap \dots \cap V_i \dots \cap V_N}{V_1 \cup V_2 \cup \dots \cup V_i \dots \cup V_N}. \quad (3)$$

The largest color diversity location is the block with the smallest $\text{IoU}_{\text{score}}$, while the smallest color diversity location is the block with the largest $\text{IoU}_{\text{score}}$. In practice, we calculate the $\text{IoU}_{\text{score}}$ on R, G, B channels separately and compute the final $\text{IoU}_{\text{score}}$ by averaging them.

Dominant Color Labels. Based on the two video blocks with the largest/smallest color diversity, we compute the corresponding dominant color labels. We divide the 3D RGB color space into 8 bins evenly and assign each bin with an index number. Then for each pixel in the video block, based on its RGB value, we assign a corresponding color bin number to it. Finally, color bin with the largest number of pixels is the label for the dominant color.

Global Appearance Statistical Labels. We also propose global appearance statistical labels to provide supplementary information. Particularly, we use the dominant color of the whole video (instead of a video block) as the global appearance statistical label. The computation method is the same as the one described above.

3.4 Curriculum Learning Strategy

We further propose to leverage the curriculum learning strategy to improve the learning performance. Curriculum learning is first proposed by Bengio *et al.* [55] in 2009 and the key concept is to present the network with more difficult samples gradually. It is inspired by the human learning process and proven to be effective on many learning tasks [20], [37], [56]. Recently, Hacoheh and Weinshall [57] further investigated the curriculum learning in training deep neural networks and proposed two fundamental problems to be resolved: (1) scoring function problem, *i.e.*, how to quantify the difficulty of each training sample; 2) pacing function problem, *i.e.*, how to feed the networks with the sorted training samples. In this work, for self-supervised video representation learning, we describe our solutions to these two problems as follows.

Scoring Function. Scoring function f defines how to measure the difficulty of each training sample. In our case, each video clip is considered to be easy or hard, based on the difficulty to figure out the block with the largest motion, *i.e.*, difficulty to regress the motion statistical labels. To characterize the difficulty, we use the ratio between magnitude sum of the largest motion block and magnitude sum of the entire videos, as the scoring function f . When the ratio is large, it indicates that the largest motion block contains the dominant action in the video and is thus easy to find out the largest motion location, *e.g.*, a man skiing in the center of a video with smooth background change. While on the other hand, when the ratio is small, it indicates that the action in the video is relatively diverse or the action is less noticeable, *e.g.*, two persons boxing with another judge walking around. See Sec. 5.4 for more visualized examples.

Formally, given an N -frame video clip, two summarized motion boundaries M_u and M_v are computed based on Eq. 2 and the corresponding magnitude maps are denoted as M_u^{mag} and M_v^{mag} . Denote the largest motion blocks as B_u , B_v and the corresponding magnitude maps as B_u^{mag} , B_v^{mag} . The scoring function f is defined as the maximum ratio between the magnitude sum of B_u , M_u and B_v , M_v :

$$f = \max\left(\frac{\sum B_u^{\text{mag}}}{\sum M_u^{\text{mag}}}, \frac{\sum B_v^{\text{mag}}}{\sum M_v^{\text{mag}}}\right). \quad (4)$$

Here we use the maximum ratio between the horizontal component u and the vertical component v . This is because large magnitude in *one* direction can already define large

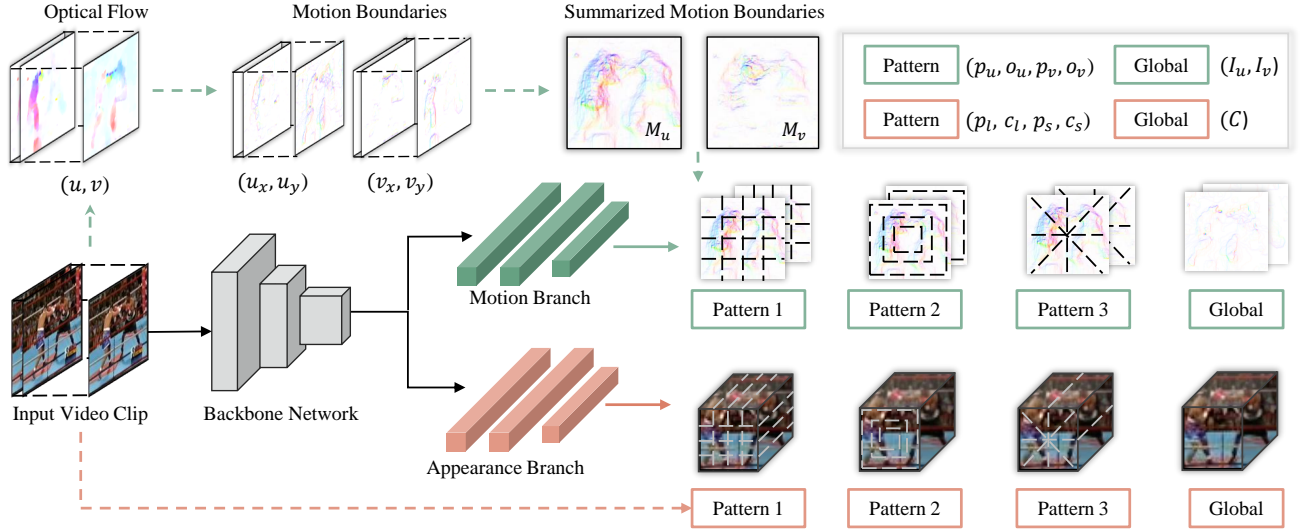


Fig. 4: The network architecture of the proposed method. Given a video clip, 14 motion statistical labels and 13 appearance statistical labels are to be regressed. The motion statistical labels are computed from summarized motion boundaries. The appearance statistical labels are computed from input video clip. For each local motion pattern, 4 ground-truth labels are generated: p_u, o_u – the spatial location of the largest magnitude based on M_u and its corresponding orientation; p_v, o_v – the spatial location of the largest magnitude based on M_v and its corresponding orientation. Two global motion statistical labels are I_u, I_v – the frame indices of the largest magnitude sum w.r.t. m_u and m_v . For each local appearance pattern, 4 ground-truth labels are generated: p_l, c_l – the spatial location of the largest color diversity and its corresponding dominant color; p_s, c_s – the spatial location of the smallest color diversity and its corresponding dominant color. The global appearance statistical label is C – the dominant color of the whole video.

motion, *e.g.*, a person running from left to right contains large motion in horizontal direction u but small motion in vertical direction v . With the scores computed from function f , training samples are sorted in a descending order accordingly, representing the difficulty from easy to hard.

Pacing Function. After sorting the samples, the remaining question is how to split these samples into different training steps. Prior works [20], [37], [56] usually adopt a two-stage training scheme, *i.e.*, training examples are divided into two categories: easy and hard. In [57], the authors formally define such a problem as a pacing function g , and introduce three stair-case functions: *single step*, *fixed exponential pacing*, and *varied exponential pacing*, where they demonstrate that these functions have comparable performances [57]. In our case, we adopt the simple single step pacing function (we also tried other functions and similarly found that they show comparable performances). Specifically, we use the first half (descendingly sorted as aforementioned) examples as easy samples and the pacing function is defined as follows:

$$g = \begin{cases} 0.5 * S, & \text{if } i < \text{step_length} \\ S, & \text{if } i \geq \text{step_length} \end{cases}, \quad (5)$$

where S is the sorted training clips, i is the training iteration, and step_length is the number of the iterations to use the entire training samples S . In practice, when the model is converged on the first half training samples, we will use the entire S for the second-stage training.

3.5 Learning with Spatio-temporal CNNs

We consider C3D [45], 3D-ResNet [58], and R(2+1)D [8] as our backbone networks to learn spatio-temporal features. In

the preliminary version [22] of this work, we use a light C3D network as described in [45]. It contains 5 convolutional layers, 5 max-pooling layers, 2 fully-connected layers, and a soft-max loss layer, which is similar to CaffeNet [59]. In this version, we further conduct extensive experiments on C3D with BN and adopt two additional modern network architectures for video analytic tasks: 3D-ResNet and R(2+1)D.

C3D [45] network extends 2D convolutional kernel $k \times k$ to 3D convolutional kernel $k \times k \times k$ to operate on 3D video volumes. It contains 5 convolutional blocks, 5 max-pooling layers, 2 fully-connected layers, and a soft-max layer in the end to predict action class. Each convolutional block contains 2 convolutional layers except the first two blocks. Batch normalization (BN) is also added between each convolutional layer and ReLU layer.

3D-ResNet [58] is a 3D extension of the widely used 2D architecture ResNet [60], which introduces shortcut connections that perform identity mapping of each building block. A basic residual block in 3D-ResNet (R3D) contains two 3D convolutional layers with BN and ReLU followed. Shortcut connection is introduced between the top of the block and the last BN layer in the block. Following previous work [58], we use 3D-ResNet18 (R3D-18) as our backbone network, which contains four basic residual blocks and one traditional convolutional block on the top.

R(2+1)D is introduced by Tran *et al.* [8] recently. It breaks the original spatio-temporal 3D convolution into a 2D spatial convolution and a 1D temporal convolution. While preserving similar network parameters to R3D, R(2+1)D outperforms R3D on the task of supervised video action recognition.

We model our self-supervised task as a regression prob-

lem. The proposed framework is illustrated in Fig. 4, where the *Backbone Network* can be replaced with each of the above-mentioned architectures and is thoroughly evaluated in the experiment (see Sec. 5.2). L_2 -norm is leveraged as the loss function to measure the difference between target statistical labels and the predicted labels. Formally, the loss function is defined as follow:

$$\mathcal{L} = \lambda_m \|\hat{y}_m - y_m\|_2 + \lambda_a \|\hat{y}_a - y_a\|_2, \quad (6)$$

where \hat{y}_m, y_m denote the predicted and target motion statistical labels, and \hat{y}_a, y_a denote the predicted and target appearance statistical labels. λ_m and λ_a are the weighting parameters that are used to balance the two loss terms.

4 EXPERIMENTAL SETUP

4.1 Datasets

We conduct extensive experimental evaluations on multiple datasets in the following sections. In Sec. 5, we validate the proposed approach through extensive ablation studies on action recognition downstream task using three datasets, Kinetics-400 [25], UCF101 [47], and HMDB51 [48]. In Sec. 6, we demonstrate the transferability of the proposed method and compare to other state-of-the-art methods on four downstream tasks, including action recognition task and video retrieval task on UCF101 and HMDB51 datasets, dynamic scene recognition task on YUPENN dataset [49], and action similarity labeling task on ASLAN dataset [61].

Kinetics-400 (K-400) [25] is a large-scale human action recognition dataset proposed recently, which contains around 306k videos of 400 action classes. It is divided into three splits: training split, validation split and testing split. Following prior work [20], we use the training split as pre-training dataset, which contains around 240k video samples.

UCF101 [47] is a widely used dataset which contains 13,320 video samples of 101 action classes. It is divided into three splits. Following prior work [14], we use the *training split 1* as self-supervised pre-training dataset and the *training/testing split 1* for downstream task evaluation.

HMDB51 [48] is a relatively small action dataset which contains around 7,000 videos of 51 action classes. This dataset is very challenging as it contains large variations in camera viewpoint, position, scale and *etc.* Following prior work [14], we use the *training/testing split 1* to evaluate the proposed self-supervised learning method.

YUPENN [49] is a dynamic scene recognition dataset which contains 420 video samples of 14 dynamic scenes. We follow the recommended leave-one-out evaluation protocol [49] when evaluating the proposed method.

ASLAN [61] is a video dataset focusing on the action similarity labeling problem and contains 3,631 video samples of 432 classes. In this work, we use it as a downstream evaluation task to validate the generality of the learned spatio-temporal representations. During testing, following prior work [61], we use a 10-fold cross validation with leave-one-out evaluation protocol.

4.2 Implementation Details

Self-supervised Pre-training Stage. When pre-training on UCF101 dataset, video samples are first split into non-

overlapped 16 frame video clips and are randomly selected during pre-training. While when pre-training on K-400, following prior works [13], [20], we randomly select a consecutive 16-frame video clip and the corresponding 15-frame optical flow clip from each video sample. Each video clip is reshaped to spatial size of 128×171 . As for data augmentation, we randomly crop the video clip to 112×112 and apply random horizontal flip for the entire video clip. Weights of motion statistics λ_m and appearance statistics λ_a are empirically set to be 1 and 0.1. The batch size is set to 30 and we use SGD optimizer with learning rate 5×10^{-4} , which is divided by 10 for every 6 epochs and the training process is stopped at 20 epochs.

Supervised Fine-tuning Stage. During the supervised fine-tuning stage, weights of convolutional layers are retained from the self-supervised pre-trained models and weights of the fully-connected layers are re-initialized. The whole network is then trained again with cross-entropy loss on action recognition task with UCF101 and HMDB51 datasets. Image pre-processing procedure and training strategy are the same as the self-supervised pre-training stage, except that the initial learning rate is changed to 0.003.

Evaluation. For action recognition task, during testing, video clips are resized to 128×171 and center-cropped to 112×112 . We consider two evaluation methods: clip accuracy and video accuracy. The clip accuracy is computed by averaging the accuracy of each clip from the testing set. While the video accuracy is computed by averaging the softmax probabilities of uniformly selected clips in each video [14] from the testing set. In all of the following experiments, to have a fair comparison with prior works [10], [14], [20], we use video accuracy to evaluate our approach, apart from the ablation studies on the effectiveness of each component (Sec. 5.1), where we use clip accuracy to keep a consistency with the previous conference paper [22].

We further evaluate the self-supervised pre-trained models by using them as feature extractors and comparing with state-of-the-art methods on many other downstream video analytic tasks, such as video retrieval, dynamic scene recognition, *etc.* This allows us to evaluate the generality of the learned spatio-temporal representations directly without fine-tuning. More evaluation details are presented in Sec. 6 for individual downstream tasks.

5 ABLATION STUDIES AND ANALYSES

In this section, we conduct extensive ablation studies to validate the proposed method and investigate four important questions: (1) How does each component proposed in our method contribute to the self-supervised video representation learning? (2) How does the type of backbone network affect the performance of downstream tasks? (3) How does the amount of pre-training data affect the self-supervised video representation learning? (4) Does the proposed curriculum learning strategy help to further improve the video representation learning?

5.1 Effectiveness of Each Component

We study the effectiveness of each component on C3D without BN in the following. The effectiveness of more powerful backbone networks is presented in Sec. 5.2.

TABLE 1: Ablation Experiments on Spatio-temporal Statistics Component.

(a) Partitioning statistical patterns		(b) Local and global statistics		(c) Motion and appearance statistics		
Initialization	UCF101(%)	Initialization	UCF101(%)	Initialization	UCF101(%)	HMDB51(%)
Random	45.4	Random	45.4	Random	45.4	19.7
Motion pattern 1	53.8	Motion global	48.3	Appearance	48.6	20.3
Motion pattern 2	53.2	Motion pattern all	55.4	Motion	57.8	30.0
Motion pattern 3	54.2	Motion pattern all + global	57.8	Joint	58.8	32.6

TABLE 2: Evaluation of three different backbone networks on the UCF101 dataset and HMDB51 dataset. When pre-training, we use our self-supervised pre-training model as weight initialization.

Experimental setup			Downstream task(%)	
Pre-training	Backbone	#Params.	UCF101	HMDB51
✗	C3D	33.4M	61.7	24.0
✓	C3D	33.4M	69.3	34.2
✗	R3D-18	14.4M	54.5	21.3
✓	R3D-18	14.4M	67.2	32.7
✗	R(2+1)D	14.4M	56.0	22.0
✓	R(2+1)D	14.4M	73.6	34.1

Pattern. We study the performances of three partitioning patterns as described in Sec. 3.2. Here, we analyze and show the performances based on the motion statistics while the appearance statistics follows the same trend. As shown in Table 1a, all three patterns achieve comparable results. When compared to random initialization, *i.e.*, training from scratch, each pattern improves by around 8%.

Local v.s. Global. We study the performances of local statistics, *where is the largest motion location?*, global statistics, *which is the largest motion frame?*, and their ensemble. As can be seen in Table 1b, when the three local patterns are combined together, we can further get around 1.5% improvement, compared to single pattern (Table 1a). The global statistics also serves as a useful supervision signal with an improvement of 3%. All motion statistics labels (all three patterns and global statistics) achieve 57.8% accuracy on the UCF101 dataset, which outperforms the random initialization by 12.4%.

Motion, RGB, and Joint Statistics. We finally analyze the performances of motion statistics, appearance statistics, and their combination, in Table 1c. It can be seen that both appearance and motion statistics serve as useful self-supervised signals for action recognition problem. But the motion statistics is more powerful as the temporal information appears to be more important for action recognition task. When combined motion and appearance statistics, the performance can be further improved.

5.2 Effectiveness of Backbone Networks

Recently, modern spatio-temporal representation learning architectures, such as R3D-18 [58] and R(2+1)D [8], have been used to validate self-supervised video representation learning methods [10], [14]. While the performances of downstream tasks are significantly improved, this practice introduces a new variable, backbone network, which could interfere with the evaluation of the pretext task itself. In the

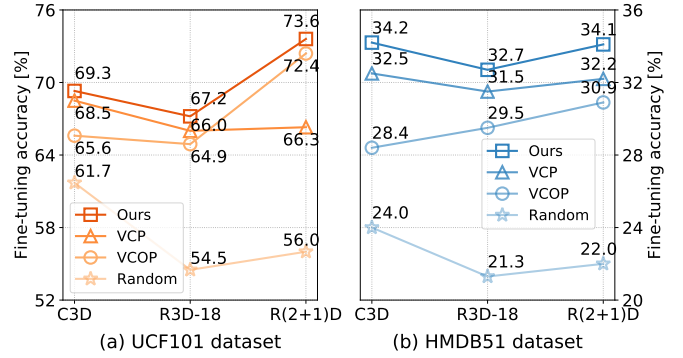


Fig. 5: Action recognition accuracy on three backbone networks (horizontal axis) using four initialization methods.

following, we first evaluate our proposed method with these modern backbone networks in Table 2. Following that, we compare our method with some recent works [10], [14] on these three network architectures, in Fig. 5.

We present the performances of different backbone networks on UCF101 and HMDB51 datasets under two settings: without pre-training and with pre-training, in Table 2. When there is no pre-training, baseline results are obtained by training from scratch on each result. When there is pre-training, backbone networks are first pre-trained on UCF101 dataset with the proposed method and then used as weights initialization for the following fine-tuning. Best performances under each setting are shown in bold. From the results we have the following observations: (1) Drastic improvement is achieved on both action recognition datasets across three backbone networks. With C3D it improves UCF101 and HMDB51 by 9.6% and 13.8%; with R3D-18 it improves UCF101 and HMDB51 by 13.6% and 12.1%; with R(2+1)D it improves UCF101 and HMDB51 by 19.5% and 15.9% remarkably. (2) Compared to C3D, R3D-18 and R(2+1)D benefit more from the self-supervised pre-training. Despite C3D achieves the best performance in the no pre-training setting, R(2+1)D finally achieves the highest accuracy on both datasets in the self-supervised setting. (3) The proposed method using (2+1)D convolution, *i.e.*, R(2+1)D, achieves better performance than using 3D convolution, *i.e.*, R3D-18, while with similar number of network parameters. Similar observation is also demonstrated in supervised action recognition task [8], where R(2+1)D performs better than R3D-18 on K-400 dataset.

We further compare our method with two recent proposed pretext tasks VCOP [14] and VCP [10] on these three backbone networks in Fig. 5. Three key observations are illustrated: (1) The proposed self-supervised learning method achieves the best performance across all three backbone networks on both UCF101 and HMDB51 datasets. This

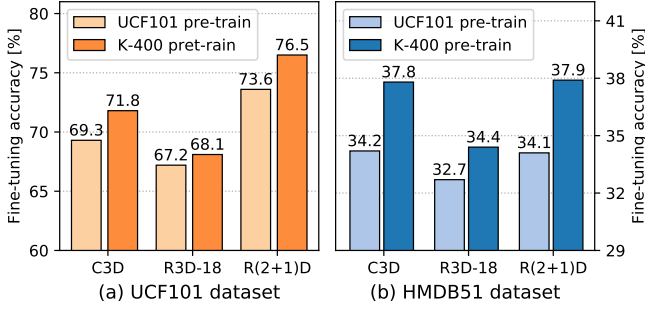


Fig. 6: Comparison of different pre-training datasets: UCF101 and K-400, across three different backbone networks on UCF101 and HMDB51 datasets.

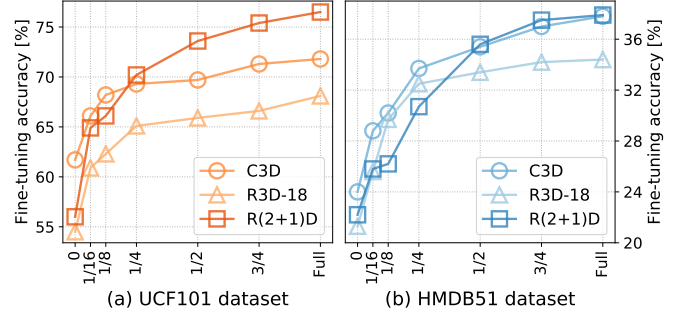


Fig. 7: Comparison of different pre-training dataset scales of K-400 across three different backbone networks. Position “0” at the x-axis indicates random initialization.

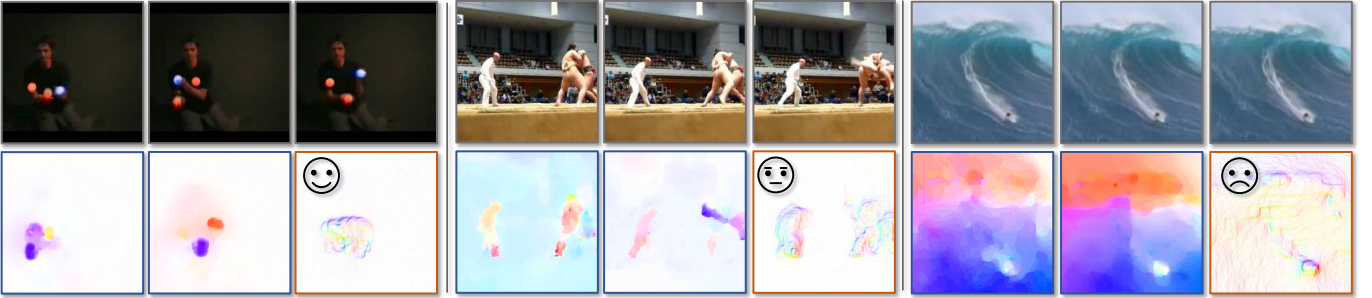


Fig. 8: Three video samples of the curriculum learning strategy. From left to right, the difficulty to regress the motion statistical labels of each video clip is increasing. For each sample, the top three images are the first, middle, and last frames of a video clip. In the bottom row, the first two images are the corresponding optical flows and the last image is the summarized motion boundaries M_u/M_v with the maximum magnitude sum.

demonstrates the superiority of our method and shows that the performance improvement is not merely due to the usage of the modern networks. The proposed spatio-temporal statistical labels indeed drive neural networks to learn powerful spatio-temporal representations for action recognition. (2) For all three pretext tasks, R(2+1)D enjoys the largest improvement (compared to *Random*) for both datasets, which is similar to the observation in the above experiments. (3) No best network architecture is guaranteed for different pretext tasks. R(2+1)D achieves the best performance with our method and VCOP, while C3D achieves the best performance with VCP.

5.3 Effectiveness of Pre-training Data

In the following, we consider two scenarios to investigate the effectiveness of pre-training data. One is comparison on different pre-training datasets with different data scales. The other is comparison on the same pre-training dataset but with different pre-training data size.

Pre-training Dataset Analysis. We analyze the performances of training on a relatively small-scale dataset UCF101 [47] and on a large-scale dataset K-400 [25]. The pre-trained models are evaluated on two downstream datasets: UCF101 and HMDB51 w.r.t. three different backbone networks as shown in Fig. 6. It can be seen that the performance could be further improved when pre-training on a larger dataset across all the backbone networks and on both downstream datasets. The effectiveness of larger dataset is also demonstrated in prior works [20], [62].

Dataset Scale Analysis. We further consider to pre-train backbone networks on different proportions of the same K-400 dataset. In practice, $1/k$ of K-400 is used for pre-training, where $k = 16, 8, 4, 2, 4/3, 1$. To obtain the corresponding pre-training dataset, for $k = 16, 8, 4, 2$, we select one sample from every k samples of the original full K-400. As for $k = 4/3$, we first retain half of the K-400, and then select one sample from every 2 samples in the remaining half dataset. We conduct extensive experiments on three backbone networks and two downstream datasets as shown in Fig. 7. It can be seen from the figure that increase of pre-training data scale does not lead to linear increase of the performance. The effectiveness of the data scale would saturate towards using the full K-400 dataset. Taking R(2+1)D as an example, compared with using full K-400, using half of the K-400 only leads to *inconsequential* drop from the highest performance. Besides, using $1/8$ of the K-400 can already achieve half of the improvement compared to training from scratch. similar observation is also demonstrated in supervised transfer learning [63]. This suggests that when considering limited computing resources, it would be important and interesting to adopt an attentive selection of the training samples.

5.4 Effectiveness of Curriculum Learning Strategy

The performances of the proposed curriculum learning strategy are shown in Table 3. Compared with the baseline results (100% K-400), the performances are further boosted on both UCF101 dataset (77.8% vs. 76.5%) and HMDB51

TABLE 3: Evaluation of the curriculum learning strategy. \uparrow represents the first half of the K-400 dataset while \downarrow indicates the last half of the K-400 dataset.

Experimental setup		Downstream tasks	
Curr. Learn.	Pre-training data	UCF101	HMDB51
\times	100 % K-400	76.5	37.9
\times	50 % K-400	73.6	35.6
\times	\uparrow , 50% K-400 (simple)	72.4	35.9
\times	\downarrow , 50% K-400 (difficult)	72.8	32.1
\checkmark	100% K-400	77.8	40.5

dataset (40.5% vs. 37.9%) , which validates the effectiveness of the proposed curriculum learning strategy. It is also interesting to note that when using the first half of the sorted training samples, *i.e.*, simple samples or the last half, *i.e.*, difficult samples, the performances on UCF101 dataset are both lower than the random half of K-400. Such observations further validate that the careful selection of training samples is of necessity in self-supervised representation learning.

Three video samples ranked from easy to hard are shown in Fig. 8. As described in Sec. 3.4, difficulty to regress the motion statistical labels is used to define the scoring function f to rank the training samples. Note that the appearance statistics labels are not considered when computing f as they demonstrate relatively limited improvement in action recognition task as shown in Table 1c.

6 COMPARISON WITH STATE-OF-THE-ARTS

In this section, we validate the proposed method both quantitatively and qualitatively, and compare with state-of-the-arts on four video understanding tasks: action recognition (Sec. 6.1), video retrieval (Sec. 6.2), dynamic scene recognition (Sec.6.3), and action similarity labeling (Sec. 6.4).

6.1 Action Recognition

Table 4 compares our method with other self-supervised learning methods on the task of action recognition. We have the following observations: (1) Compared with random initialization (training from scratch), networks fine-tuned on pre-trained models with the proposed self-supervised method achieve significant improvement on both UCF101 (77.8% vs. 56%) and HMDB51 (40.5% vs. 22.0%). Such results demonstrate the great potential of self-supervised video representation learning. (2) Our method achieves state-of-the-art performance on both datasets, improving UCF101 by 2.1% and HMDB51 by 4.8% compared with DPC [20]. Note that the input size of DPC is 224×224 and when considering the same input size 112×112 as ours, the proposed method improves DPC on UCF101 by 9.6%. (3) Similar to the observation in Sec. 5.2, besides pretext tasks, backbone networks also play an important role in self-supervised video representation learning. For example, pretext tasks using 3D neural networks significantly outperforms those using 2D neural networks.

Attention Visualization. Fig. 9 visualizes the attention maps on several video samples using [65]. For action classes with subtle differences, *e.g.*, *Apply lipstick* and *Apply eye*

TABLE 4: Comparison with state-of-the-art self-supervised learning methods on the action recognition task. * indicates that the input spatial size is 224×224 .

Method	Pre-training			Evaluation	
	Backbone	#Params.	Dataset	UCF101	HMDB51
Random	R(2+1)D	14.4M	-	56.0	22.0
Fully supervised	R(2+1)D	14.4M	K-400	93.1	63.6
Object Patch [34]	AlexNet	62.4M	UCF101	42.7	15.6
ClipOrder [11]	CaffeNet	58.3M	UCF101	50.9	19.8
Deep RL [9]	CaffeNet	58.3M	UCF101	58.6	25.0
OPN [12]	VGG	8.6M	UCF101	59.8	23.8
VCP [10]	C3D	34.4M	UCF101	68.5	32.5
VCOP [14]	R(2+1)D	14.4M	UCF101	72.4	30.9
RotNet3D [64]	R3D-18	33.6M	K-400	62.9	33.7
ST-puzzle [13]	R3D-18	33.6M	K-400	65.8	33.7
DPC [20]	R3D-18	14.2M	K-400	68.2	34.5
DPC* [20]	R3D-34	32.6M	K-400	75.7	35.7
Ours	R(2+1)D	14.4M	K-400	76.5	37.9
Ours (CL)	R(2+1)D	14.4M	K-400	77.8	40.5

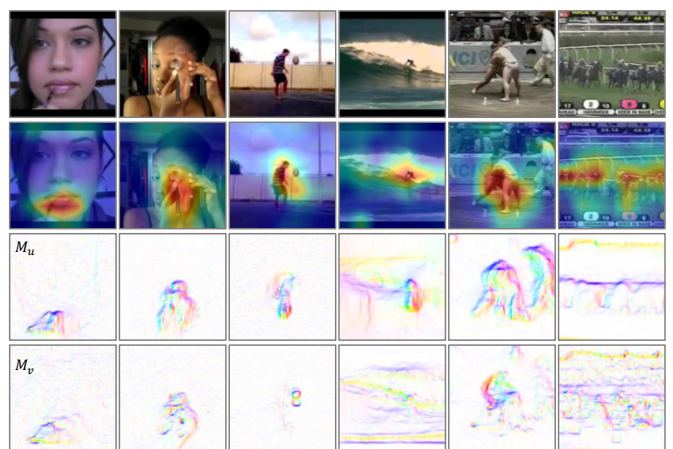


Fig. 9: Attention visualization. For each sample from top to bottom: A frame from a video clip, activation based attention map of conv5 layer on the frame by using [65], summarized motion boundaries M_u , and summarized motion boundaries M_v computed from the video clip.

makeup, the pre-trained model is sensitive to the location that is exactly the largest motion location as quantified by the summarized motion boundaries M_u and M_v . It is also interesting to note that for the *SumoWrestling* video sample (the fifth column), although three persons (two players and one judge) have large motion in direction u , only players demonstrate larger motion in direction v . As a result, the attention map is mostly activated around the players.

The performances on the action recognition downstream task strongly validate the great power of self-supervised learning methods. The proposed pretext task is demonstrated to be effective in driving backbone networks to learn spatio-temporal features for action recognition. While to the goal of learning generic features, it is also important and interesting to evaluate the absolute effect of the learned features without fine-tuning on the downstream task. In the following, we directly evaluate the features on three different problems by using the networks as feature extractors.

6.2 Video Retrieval

We evaluate spatio-temporal representations learned from the self-supervised method on video retrieval task. Fol-

TABLE 5: Comparison with state-of-the-art self-supervised learning methods on the video retrieval task with the UCF101 dataset. The best results from pool5 w.r.t. each 3D backbone network are shown in **bold**. The results from pool4 on our method are in *italic* and highlighted.

	Method	Top1	Top5	Top10	Top20	Top50
AlexNet	Jigsaw [28]	19.7	28.5	33.5	40.0	49.4
	OPN [12]	19.9	28.7	34.0	40.6	51.6
	Deep RL [9]	25.7	36.2	42.2	49.2	59.5
C3D	Random	16.7	27.5	33.7	41.4	53.0
	VCOP [14]	12.5	29.0	39.0	50.6	66.9
	VCP [10]	17.3	31.5	42.0	52.6	67.7
	Ours	20.5	39.6	50.8	62.2	76.7
	<i>Ours (p4)</i>	<i>30.1</i>	<i>49.6</i>	<i>58.8</i>	<i>67.6</i>	<i>78.5</i>
R3D-18	Random	9.9	18.9	26.0	35.5	51.9
	VCOP [14]	14.1	30.3	40.4	51.1	66.5
	VCP [10]	18.6	33.6	42.5	53.5	68.1
	Ours	23.9	43.9	54.3	64.9	78.2
	<i>Ours (p4)</i>	<i>28.7</i>	<i>47.7</i>	<i>58.3</i>	<i>67.8</i>	<i>78.5</i>
R(2+1)D	Random	10.6	20.7	27.4	37.4	53.1
	VCOP [14]	10.7	25.9	35.4	47.3	63.9
	VCP [10]	19.9	33.7	42.0	50.5	64.4
	Ours	21.2	40.1	51.5	62.5	77.1
	<i>Ours (p4)</i>	<i>26.2</i>	<i>45.9</i>	<i>56.5</i>	<i>66.3</i>	<i>78.4</i>

lowed [10], [14], given a video, ten 16-frame clips are first sampled uniformly. Then the video clips are fed into the self-supervised pre-trained models to extract features from the last pooling layer (pool5). Based on the extracted video features, cosine distances between videos of testing split and training split are computed. Finally, the video retrieval performance is evaluated on the testing split by querying Top- k nearest neighbours from the training split based on cosine distances. Here, we consider k to be 1, 5, 10, 20, 50. If the test clip class label is within the Top- k retrieval results, it is considered to be successfully retrieved.

Table 5 and Table 6 compare our method with other self-supervised learning methods on UCF101 dataset and HMDB51 dataset, respectively. It can be seen that our method achieves the state-of-the-art results and outperforms VCOP [14] and VCP [10] on both datasets across three different backbone networks (shown in bold). We are interested in if the performances could be further improved, as the video features extracted from the pool5 layer tend to be more task-specific while lack generalizability for the retrieval downstream task. To validate this hypothesis, we extract video features from all the preceding pooling layers and evaluate them on the video retrieval task. Typically, we compare the self-supervised method (pre-trained on the proposed pretext task) and supervised method (pre-trained on the action labels) on HMDB51 dataset in Fig. 10 (UCF101 dataset follows the similar trend).

We have the following key observations: (1) In our self-supervised method, with the evaluation layer going deeper, the retrieval performance would increase to a peak (usually at pool3 or pool4 layer) and then decrease. Similar observation is also reported in self-supervised image representation learning [66]. The corresponding performance of pool4 layer is reported in Table 5 and Table 6 (highlighted in blue).

TABLE 6: Comparison with state-of-the-art self-supervised learning methods on the video retrieval task with the HMDB51 dataset. The best results from pool5 w.r.t. each 3D backbone network are shown in **bold**. The results from pool4 on our method are in *italic* and highlighted.

	Method	Top1	Top5	Top10	Top20	Top50
C3D	Random	7.4	20.5	31.9	44.5	66.3
	VCOP [14]	7.4	22.6	34.4	48.5	70.1
	VCP [10]	7.8	23.8	35.5	49.3	71.6
	Ours	10.6	26.1	39.7	55.0	77.2
	<i>Ours (p4)</i>	<i>13.9</i>	<i>33.3</i>	<i>44.7</i>	<i>59.5</i>	<i>78.1</i>
R3D-18	Random	6.7	18.3	28.3	43.1	67.9
	VCOP [14]	7.6	22.9	34.4	48.8	68.9
	VCP [10]	7.6	24.4	36.6	53.6	76.4
	Ours	11.8	30.1	41.2	56.9	78.4
	<i>Ours (p4)</i>	<i>14.2</i>	<i>32.2</i>	<i>44.1</i>	<i>60.2</i>	<i>81.3</i>
R(2+1)D	Random	4.5	14.8	23.4	38.9	63.0
	VCOP [14]	5.7	19.5	30.7	45.8	67.0
	VCP [10]	6.7	21.3	32.7	49.2	73.3
	Ours	9.9	25.9	37.9	54.6	77.8
	<i>Ours (p4)</i>	<i>12.1</i>	<i>30.0</i>	<i>41.4</i>	<i>56.7</i>	<i>78.0</i>

(2) R3D-18 is more robust to such performance decline as its turning point occurs at pool4 layer while others usually occur at pool3 layers, especially on the Top-20 and Top-50 experiments. (3) Our self-supervised method significantly outperforms the supervised method, especially at deeper layers. This suggests that features learned from our self-supervised method are more robust and generic when transferring to the video retrieval task. Some qualitative video retrieval results are shown in Fig. 11.

6.3 Dynamic Scene Recognition

We further study the transferability of the learned features on dynamic scene recognition problem with the YUPENN dataset [49], which contains 420 video samples of 14 dynamic scenes. Following prior work [45], each video sample is first split into 16-frame clips with 8 frames overlapped. Then the spatio-temporal feature of each clip is extracted based on the self-supervised pre-trained models from pooling layers. In practice, similar to Sec. 6.2, we investigate the best-performing pooling layer w.r.t. each backbone network in such a problem, where for C3D and R(2+1)D, the best-performing layer is *pool3*; for R3D-18, the best-performing layer is *pool4*. Next, video-level representations are obtained by averaging the corresponding video-clip features, followed by L_2 normalization. Finally, a linear SVM is used for classification and we follow the same leave-one-out evaluation protocol as described in [49].

We compare our approach with state-of-the-art hand-crafted features and other self-supervised learning methods in Table 7. It can be seen from the table that the proposed method significantly outperforms the second best self-supervised learning method Geometry [16] by 9.8%, 6.9%, and 6.2% w.r.t. C3D, R3D-18, and R(2+1)D backbone networks, respectively. Besides, our method also outperforms the best hand-crafted feature BoSE [51] by 0.5%. Note that BoSE combined different sophisticated feature encodings (FV, LLC and dynamic pooling) while we only use average

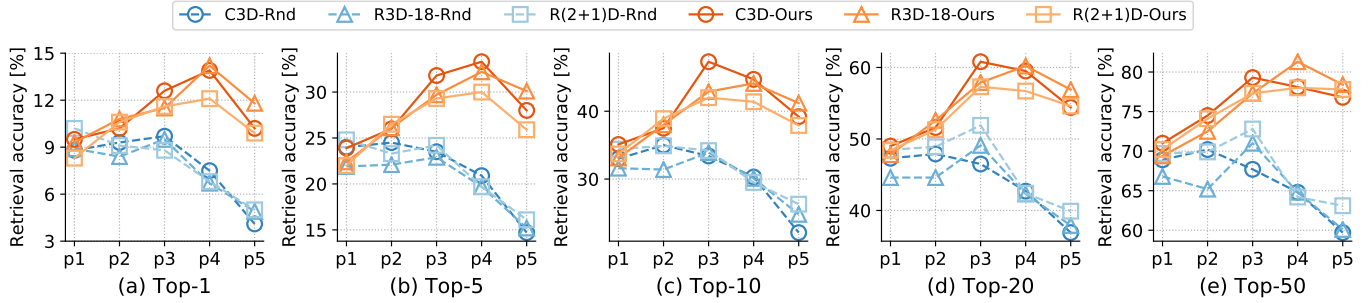


Fig. 10: Evaluation of features from different stages of the network, *i.e.*, pooling layers, on the video retrieval task with the HMDB51 dataset. The dotted blue lines show the performances of the supervised pre-trained models on the action recognition problem, *i.e.*, random initialization (Rnd). The orange lines show the performances of the self-supervised pre-trained models with our method (Ours). Better visualization with color.



Fig. 11: From top to bottom: three qualitative examples of video retrieval on the UCF101 dataset. From left to right: one query frame from the testing split, frames from the top-3 retrieval results based on the supervised pre-trained models, and frames from the top-3 retrieval results based on our self-supervised pre-trained models. The correctly retrieved results are marked in blue while the failure cases are in orange. Better visualization with color.

TABLE 7: Comparison with state-of-the-art hand-crafted methods and self-supervised representation learning methods on the dynamic scene recognition task.

Method	Hand-crafted	Self-supervised	YUPENN
SOE [49]	✓		80.7
SFA [50]	✓		85.5
BoSE [51]	✓		96.2
Object Patch [34]		✓	70.5
ClipOrder [11]		✓	76.7
Geometry [16]		✓	86.9
Ours, C3D		✓	96.7
Ours, R3D-18		✓	93.8
Ours, R(2+1)D		✓	93.1

pooling with a *linear* SVM. It is therefore demonstrated that the spatio-temporal features learned from the proposed self-supervised learning method have impressive transferability.

6.4 Action Similarity Labeling

In this section we introduce a challenging downstream task – action similarity labeling. The learned spatio-temporal representations are evaluated on the ASLAN dataset [61], which contains 3,631 video samples of 432 classes. Unlike

TABLE 8: Comparison with different hand-crafted features and fully-supervised models on the ASLAN dataset.

Features	Hand-crafted	Sup.	Self-sup.	Acc.
C3D [45]		✓		78.3
P3D [46]		✓		80.8
HOF [61]	✓			56.7
HNF [61]	✓			59.5
HOG [61]	✓			59.8
Ours, C3D			✓	60.9
Ours, R3D-18			✓	60.9
Ours, R(2+1)D			✓	61.6

action recognition task or dynamic scene recognition task that aims to predict the actual class label, the action similarity labeling task focuses on the *similarity* of two actions instead of the actual class label. That is, given two video samples, the goal is to predict whether the two samples are of the same class or not. This task is quite challenging as the test set contains *never-before-seen* actions [61].

To evaluate on the action similarity labeling task, we use the self-supervised pre-trained models as feature extractors and use a *linear* SVM for the binary classification, following prior work [45]. Specifically, given a pair of videos, each

video sample is first split into 16-frame clips with 8 frames overlapped and then fed into the network to extract features from the pool3, pool4 and pool5 layers. The video-level spatio-temporal feature is obtained by averaging the clip features, followed by L_2 normalization. After extracting three types of features for each video, we then compute 12 different distances for each feature as described in [61]. The three 12 (dis-)similarities are concatenated together to obtain a 36-dimensional feature. Since the scales of each distance are different, we normalize the distances separately into zero-mean and unit-variance, following [45]. A linear SVM is used for classification and we use the 10-fold leave-one-out cross validation same as [45], [61].

Table 8 compares our method with full-supervised methods and hand-crafted features. We set a new baseline for the self-supervised method as no previous self-supervised learning methods have been validated on this task. We have the following observations: (1) Our method outperforms the hand-crafted features: HOF, HOG, and HNF(a composition of HOG and HOF). While there is still a big gap between the full supervised method. (2) Unlike the observations in previous experiments (*e.g.*, action recognition), the performances of the three backbone networks are comparable with each other. We suspect the reason lies on the fine-tuning scheme leveraged in previous evaluation protocols, where the backbone architecture plays an important role. As a result, we suggest that the proposed evaluation on the ASLAN dataset (Table 8) could serve as a complementary evaluation task for self-supervised video representation learning to alleviate the influence of backbone networks.

7 CONCLUSIONS

In this work, we presented a novel approach for self-supervised video representation learning by regressing a set of spatio-temporal labels derived from motion and appearance statistics. A curriculum learning strategy was incorporated to further improve the representation learning performance. To validate the effectiveness of our method, we conducted extensive experiments on four downstream tasks of action recognition, video retrieval, dynamic scene recognition, and action similarity labeling, over three different backbone networks, C3D, R3D-18 and R(2+1)D. Our method is shown to achieve state-of-the-art performance on various datasets accordingly. When directly evaluating the learned features by using the pre-trained models as feature extractors, our approach demonstrates great robustness and transferability to the downstream tasks and significantly outperforms the competing self-supervised methods.

It is demonstrated in recent works that larger input video size [20], longer input video length [64] and a more powerful backbone network [67] could further improve the self-supervised video representation learning. It would be interesting to extend the current method to these experimental settings. Another promising direction is to incorporate conventional machine learning methods and explore their effectiveness for self-supervised learning. For instance, we use the traditional MBH to compute the pretext task labels and validate its superiority over the other self-supervised learning methods. Some recent studies [68], [69] also demonstrate that the extension of traditional Noise-Contrastive

Estimation [70] in contrastive learning achieves promising results in self-supervised visual representation learning.

ACKNOWLEDGMENTS

This work is partially supported by the Hong Kong RGC TRS under T42-409/18-R, the Hong Kong ITC under Grant ITS/448/16FP, the VC Fund 4930745 of the CUHK T Stone Robotics Institute, and the EPSRC Programme Grant See-bibyte EP/M013774/1.

REFERENCES

- [1] J. Carreira and A. Zisserman, "Quo vadis, action recognition? a new model and the kinetics dataset," in *CVPR*, 2017.
- [2] D. Tran, H. Wang, L. Torresani, J. Ray, Y. LeCun, and M. Paluri, "A closer look at spatiotemporal convolutions for action recognition," in *CVPR*, 2018.
- [3] Y. Liu, S. Albanie, A. Nagrani, and A. Zisserman, "Use what you have: Video retrieval using representations from collaborative experts," *arXiv preprint arXiv:1907.13487*, 2019.
- [4] A. Miech, D. Zhukov, J.-B. Alayrac, M. Tapaswi, I. Laptev, and J. Sivic, "Howto100m: Learning a text-video embedding by watching hundred million narrated video clips," in *ICCV*, 2019.
- [5] B. Wang, L. Ma, W. Zhang, and W. Liu, "Reconstruction network for video captioning," in *CVPR*, 2018.
- [6] J. Wang, W. Jiang, L. Ma, W. Liu, and Y. Xu, "Bidirectional attentive fusion with context gating for dense video captioning," in *CVPR*, 2018.
- [7] K. Simonyan and A. Zisserman, "Two-stream convolutional networks for action recognition in videos," in *NeurIPS*, 2014.
- [8] D. Tran, H. Wang, L. Torresani, J. Ray, Y. LeCun, and M. Paluri, "A closer look at spatiotemporal convolutions for action recognition," in *CVPR*, 2018.
- [9] U. Buchler, B. Brattoli, and B. Ommer, "Improving spatiotemporal self-supervision by deep reinforcement learning," in *ECCV*, 2018.
- [10] D. Luo, C. Liu, Y. Zhou, D. Yang, C. Ma, Q. Ye, and W. Wang, "Video cloze procedure for self-supervised spatio-temporal learning," *arXiv preprint arXiv:2001.00294*, 2020.
- [11] I. Misra, C. L. Zitnick, and M. Hebert, "Shuffle and learn: unsupervised learning using temporal order verification," in *ECCV*, 2016.
- [12] H.-Y. Lee, J.-B. Huang, M. Singh, and M.-H. Yang, "Unsupervised representation learning by sorting sequences," in *ICCV*, 2017.
- [13] D. Kim, D. Cho, and I. S. Kweon, "Self-supervised video representation learning with space-time cubic puzzles," in *AAAI*, 2019.
- [14] D. Xu, J. Xiao, Z. Zhao, J. Shao, D. Xie, and Y. Zhuang, "Self-supervised spatiotemporal learning via video clip order prediction," in *CVPR*, 2019.
- [15] B. Fernando, H. Bilen, E. Gavves, and S. Gould, "Self-supervised video representation learning with odd-one-out networks," in *CVPR*, 2017.
- [16] C. Gan, B. Gong, K. Liu, H. Su, and L. J. Guibas, "Geometry guided convolutional neural networks for self-supervised video representation learning," in *CVPR*, 2018.
- [17] C. Vondrick, H. Pirsiavash, and A. Torralba, "Generating videos with scene dynamics," in *NeurIPS*, 2016.
- [18] W. Lotter, G. Kreiman, and D. Cox, "Deep predictive coding networks for video prediction and unsupervised learning," *arXiv preprint arXiv:1605.08104*, 2016.
- [19] M. Mathieu, C. Couprie, and Y. LeCun, "Deep multi-scale video prediction beyond mean square error," in *ICLR*, 2016.
- [20] T. Han, W. Xie, and A. Zisserman, "Video representation learning by dense predictive coding," in *ICCV Workshops*, 2019.
- [21] M. A. Giese and T. Poggio, "Cognitive neuroscience: neural mechanisms for the recognition of biological movements," *Nature Reviews Neuroscience*, vol. 4, no. 3, pp. 179–192, 2003.
- [22] J. Wang, J. Jiao, L. Bao, S. He, Y. Liu, and W. Liu, "Self-supervised spatio-temporal representation learning for videos by predicting motion and appearance statistics," in *CVPR*, 2019.
- [23] L. Jing and Y. Tian, "Self-supervised visual feature learning with deep neural networks: A survey," *IEEE Transactions on Pattern Analysis and Machine Intelligence*, 2020.
- [24] J. Deng, W. Dong, R. Socher, L.-J. Li, K. Li, and L. Fei-Fei, "Imagenet: A large-scale hierarchical image database," in *CVPR*, 2009.

- [25] W. Kay, J. Carreira, K. Simonyan, B. Zhang, C. Hillier, S. Vijayanarasimhan, F. Viola, T. Green, T. Back, P. Natsev *et al.*, “The kinetics human action video dataset,” *arXiv preprint arXiv:1705.06950*, 2017.
- [26] A. Karpathy, G. Toderici, S. Shetty, T. Leung, R. Sukthankar, and L. Fei-Fei, “Large-scale video classification with convolutional neural networks,” in *CVPR*, 2014.
- [27] C. Doersch, A. Gupta, and A. A. Efros, “Unsupervised visual representation learning by context prediction,” in *ICCV*, 2015.
- [28] M. Noroozi and P. Favaro, “Unsupervised learning of visual representations by solving jigsaw puzzles,” in *ECCV*, 2016.
- [29] R. Zhang, P. Isola, and A. A. Efros, “Colorful image colorization,” in *ECCV*, 2016.
- [30] D. Pathak, P. Krahenbuhl, J. Donahue, T. Darrell, and A. A. Efros, “Context encoders: Feature learning by inpainting,” in *CVPR*, 2016.
- [31] M. Noroozi, H. Pirsiavash, and P. Favaro, “Representation learning by learning to count,” in *ICCV*, 2017.
- [32] S. Gidaris, P. Singh, and N. Komodakis, “Unsupervised representation learning by predicting image rotations,” in *ICLR*, 2018.
- [33] M. Caron, P. Bojanowski, A. Joulin, and M. Douze, “Deep clustering for unsupervised learning of visual features,” in *ECCV*, 2018.
- [34] X. Wang and A. Gupta, “Unsupervised learning of visual representations using videos,” in *ICCV*, 2015.
- [35] D. Pathak, R. B. Girshick, P. Dollár, T. Darrell, and B. Hariharan, “Learning features by watching objects move,” in *CVPR*, 2017.
- [36] A. Owens and A. A. Efros, “Audio-visual scene analysis with self-supervised multisensory features,” in *ECCV*, 2018.
- [37] B. Korbar, D. Tran, and L. Torresani, “Cooperative learning of audio and video models from self-supervised synchronization,” in *NeurIPS*, 2018.
- [38] N. Hussein, E. Gavves, and A. W. Smeulders, “Timeception for complex action recognition,” in *CVPR*, 2019.
- [39] Y.-W. Chao, S. Vijayanarasimhan, B. Seybold, D. A. Ross, J. Deng, and R. Sukthankar, “Rethinking the faster r-cnn architecture for temporal action localization,” in *CVPR*, 2018.
- [40] Z. Shou, J. Chan, A. Zareian, K. Miyazawa, and S.-F. Chang, “Cdc: Convolutional-de-convolutional networks for precise temporal action localization in untrimmed videos,” in *CVPR*, 2017.
- [41] Z. Shou, D. Wang, and S.-F. Chang, “Temporal action localization in untrimmed videos via multi-stage cnns,” in *CVPR*, 2016.
- [42] I. Laptev, “On space-time interest points,” *International Journal on Computer Vision*, vol. 64, no. 2-3, pp. 107–123, 2005.
- [43] A. Klaser, M. Marszałek, and C. Schmid, “A spatio-temporal descriptor based on 3d-gradients,” in *BMVC*, 2008.
- [44] H. Wang and C. Schmid, “Action recognition with improved trajectories,” in *ICCV*, 2013.
- [45] D. Tran, L. Bourdev, R. Fergus, L. Torresani, and M. Paluri, “Learning spatiotemporal features with 3d convolutional networks,” in *ICCV*, 2015.
- [46] Z. Qiu, T. Yao, and T. Mei, “Learning spatio-temporal representation with pseudo-3d residual networks,” in *ICCV*, 2017.
- [47] K. Soomro, A. R. Zamir, and M. Shah, “Ucf101: A dataset of 101 human actions classes from videos in the wild,” *arXiv preprint arXiv:1212.0402*, 2012.
- [48] H. Kuehne, H. Jhuang, E. Garrote, T. Poggio, and T. Serre, “Hmdb: a large video database for human motion recognition,” in *ICCV*, 2011.
- [49] K. G. Derpanis, M. Lecce, K. Daniilidis, and R. P. Wildes, “Dynamic scene understanding: The role of orientation features in space and time in scene classification,” in *CVPR*, 2012.
- [50] C. Thierault, N. Thome, and M. Cord, “Dynamic scene classification: Learning motion descriptors with slow features analysis,” in *CVPR*, 2013.
- [51] C. Feichtenhofer, A. Pinz, and R. P. Wildes, “Bags of spacetime energies for dynamic scene recognition,” in *CVPR*, 2014.
- [52] T. Brox, A. Bruhn, N. Papenberg, and J. Weickert, “High accuracy optical flow estimation based on a theory for warping,” in *ECCV*, 2004.
- [53] N. Dalal, B. Triggs, and C. Schmid, “Human detection using oriented histograms of flow and appearance,” in *ECCV*, 2006.
- [54] H. Wang, A. Kläser, C. Schmid, and C.-L. Liu, “Action recognition by dense trajectories,” in *CVPR*, 2011.
- [55] Y. Bengio, J. Louradour, R. Collobert, and J. Weston, “Curriculum learning,” in *ICML*, 2009.
- [56] O. Sumer, T. Dencker, and B. Ommer, “Self-supervised learning of pose embeddings from spatiotemporal relations in videos,” in *ICCV*, 2017.
- [57] G. Hachohen and D. Weinshall, “On the power of curriculum learning in training deep networks,” in *ICML*, 2019.
- [58] K. Hara, H. Kataoka, and Y. Satoh, “Can spatiotemporal 3d cnns retrace the history of 2d cnns and imagenet?” in *CVPR*, 2018.
- [59] Y. Jia, E. Shelhamer, J. Donahue, S. Karayev, J. Long, R. Girshick, S. Guadarrama, and T. Darrell, “Caffe: Convolutional architecture for fast feature embedding,” in *ACM Multimedia*, 2014.
- [60] K. He, X. Zhang, S. Ren, and J. Sun, “Deep residual learning for image recognition,” in *CVPR*, 2016.
- [61] O. Kliper-Gross, T. Hassner, and L. Wolf, “The action similarity labeling challenge,” *IEEE Transactions on Pattern Analysis and Machine Intelligence*, vol. 34, no. 3, pp. 615–621, 2011.
- [62] H. Alwassel, D. Mahajan, L. Torresani, B. Ghanem, and D. Tran, “Self-supervised learning by cross-modal audio-video clustering,” *arXiv preprint arXiv:1911.12667*, 2019.
- [63] M. Huh, P. Agrawal, and A. A. Efros, “What makes imagenet good for transfer learning?” *arXiv preprint arXiv:1608.08614*, 2016.
- [64] L. Jing, X. Yang, J. Liu, and Y. Tian, “Self-supervised spatiotemporal feature learning via video rotation prediction,” *arXiv preprint arXiv:1811.11387*, 2018.
- [65] S. Zagoruyko and N. Komodakis, “Paying more attention to attention: Improving the performance of convolutional neural networks via attention transfer,” in *ICLR*, 2017.
- [66] A. Kolesnikov, X. Zhai, and L. Beyer, “Revisiting self-supervised visual representation learning,” in *CVPR*, 2019.
- [67] B. Sagie, E. Ariel, L. Oran, M. Inbar, W. T. Freeman, R. Michael, I. Michal, and D. Tali, “Speednet: learning the speediness in videos,” in *CVPR*, 2020.
- [68] A. v. d. Oord, Y. Li, and O. Vinyals, “Representation learning with contrastive predictive coding,” *arXiv preprint arXiv:1807.03748*, 2018.
- [69] T. Chen, S. Kornblith, M. Norouzi, and G. Hinton, “A simple framework for contrastive learning of visual representations,” *arXiv preprint arXiv:2002.05709*, 2020.
- [70] M. U. Gutmann and A. Hyvärinen, “Noise-contrastive estimation of unnormalized statistical models, with applications to natural image statistics,” *Journal of Machine Learning Research*, vol. 13, no. Feb, pp. 307–361, 2012.